

BSS/⁶LiI Response Matrix to neutrons from 2.5E(-8) to 100 MeV

Héctor René Vega-Carrillo and Eduardo Manzanares-Acuña
Unidades Académicas de Estudios Nucleares e Ingeniería Eléctrica
Universidad Autónoma de Zacatecas
Apdo. Postal # 336, 98000 Zacatecas, Zac. México
fermineutron@yahoo.com, emanz_44@yahoo.com

Eduardo Gallego and Alfredo Lorente
Departamento de Ingeniería Nuclear
Universidad Politécnica de Madrid
José Gutiérrez Abascal 2
28006 Madrid, Spain

M.P. Iñiguez, A. Martín-Martín and J.L. Gutiérrez-Villanueva
Departamento de Física Teórica, Atómica y Óptica
Laboratorio LIBRA
Universidad de Valladolid, Spain

Abstract

Using Monte Carlo methods the response matrix of a Bonner sphere spectrometer was calculated. As thermal neutron detector a 0.4 cm × Ø 0.4 cm ⁶LiI was utilized. The response functions were calculated for 0, 2, 3, 5, 8, 10, and 12 inches-diameter polyethylene spheres. Twenty three monoenergetic neutron sources ranging from 2.50E(-8) to 100 MeV were used and the resulting response functions were interpolated to 51 neutron energies. These were compared with a matrix response reported in the literature that was previously scaled by a factor that make corrections for the scintillator features utilized in this study and the response matrix reported in the literature. In this comparison both response matrices are in agreement. The main differences were found in the bare detector case, these are attributed to the differences in the irradiation conditions and cross sections libraries utilized in both studies. For the other detectors the differences are due to the cross sections.

1. INTRODUCTION

In 1932 Chadwick did probe the existence of neutrons [1], nowadays these particles are an important tool in science and technology. In 1960 the multisphere spectrometer, also known as Bonner sphere spectrometer (BSS), was invented with the purpose to measure both, the neutron flux and the neutron energy distribution known as neutron spectrum [2]. BSS is a set of polyethylene spheres with different diameters with a thermal neutron detector that is alternatively

located at the centre of the spheres. The use of polyethylene spheres is to reduce the energy of incoming neutrons in order to reach the detector as thermal neutrons. Due to spheres geometry the response of BSS is isotropic. From 1960 to 1979 several advances in computer unfolding methods, the application of semiconductor detectors to neutron spectrometry and the introduction of superheated drop detectors contributed to progress in neutron spectrometry [3].

With the BSS the neutron spectra is obtained in a pervasive interval of energies ranging from thermal up to at least 20 MeV [4]. The inclusion of intermediate shells of lead to the spheres habilitates the BSS to measure neutrons with larger energies [5, 6].

Different materials had been utilized as thermal neutron detector in the BSS such as, ⁶LiI(Eu) scintillator [2, 7], pairs of thermoluminescent dosimeters (TLD600-TLD700) [8-10], activation foils, like Au and In [11], track detectors [12], BF₃ [13] and ³He [14] proportional counters. The efficiency of any of these detectors is larger for thermal neutrons; this efficiency is the response function of the bare detector. When the thermal neutron detector is located inside of any polyethylene sphere its response function is defined by the sphere diameter. Thus, the set of response functions becomes the BSS response matrix [6, 15].

Inside a neutron radiation field the detector, bare or inside of any sphere, produces a count rate (C); these are related with the response matrix (R_Φ(E)) and the neutron spectrum (Φ_E(E)) through the Fredholm integral equation of the first kind, shown in equation 1.

$$C = \int_{E_i}^{E_f} R_{\Phi}(E) \Phi_E(E) dE \quad (1)$$

Once equation 1 is solved and the neutron spectrum is known the neutron dose (Δ) can be estimated using equation 2 [16].

$$\Delta = \int_{E_i}^{E_f} \delta_{\Phi}(E) \Phi_E(E) dE \quad (2)$$

Here, δ_Φ(E) is the fluence-to-dose conversion coefficients. Depending of the type of δ_Φ(E) utilized any type of neutron dose can be estimated.

Technological limitations prevent the experimental determination of the response matrix utilizing monoenergetic neutrons. However, this is only practical for few monoenergetic neutrons with energies greater than about a few keV and for thermal neutrons [6]. Therefore the responses are currently estimated through calculations. Thus, response matrices have been calculated solving the transport equation or using Monte Carlo Methods. The response matrix of BSS with ⁶LiI(Eu) (BSS/⁶LiI(Eu)) has been calculated with the ANISIN code [17] and using the MCNP [18, 19], MCNPX [14] codes as well as other high-energy codes [5]. The reason of these efforts is to

improve the accuracy of the response matrix. Because in each calculation are including the updated cross section data as well as the accuracy of BSS model.

In this study the response matrix of a Bonner spectrometer with a ^6LiI scintillator to neutrons with energies from $2.5\text{E}(-8)$ to 100 MeV has been calculated using Monte Carlo methods. The response was obtained using updated cross section libraries. Calculated matrix was interpolated to include a larger number of energy bins and it was compared with the response matrix reported in the literature.

2. METHODS

Along the calculations a realistic model of the detector was designed, this includes a $0.4\text{ cm} \times 0.4\text{ cm}$ ^6LiI scintillator, the light pipes and the detector's cask, and the polyethylene spheres. The calculated cases were the bare detector (Ball 0) and those with the detector inserted in the spheres of 2" (Ball 2), 3" (Ball 3), 5" (Ball 5), 8" (Ball 8), 10" (Ball 10) and 12" (Ball 12). In the model definition the light pipes were modeled as made of polymethyl methacrylate, the cask was modeled as made of aluminum and the scintillator was modeled as made of ^6Li , ^7Li and I; the Eu impurities were excluded.

Each model was irradiated with a parallel neutron beam produced by a disk-shaped neutron source; irradiations were carried out using 20 monoenergetic neutrons for each detector. The energy of the monoenergetic neutron sources varied from $2.50\text{E}(-8)$ to 20 MeV. These calculations were performed with the Monte Carlo code MCNP 4C [20] and the ENDF/B-VI cross section library [21].

Using MCNPX [22], version 2.4.0, the response calculations were extended until 100 MeV neutrons using the LA150 cross section library [23]. In all calculations the response was defined as the number of $^6\text{Li}(n, \alpha)^3\text{H}$ reactions occurring in the ^6LiI scintillator per each neutron emitted by the disk-shaped monoenergetic neutron source.

In the calculations reported in literature the scintillator has been modeled with different densities, 4.05 g-cm^{-3} [18] and 4.08 g-cm^{-3} [24], and with different concentrations of ^6Li isotope. The enrichment in ^6Li utilized has been 96.1% [18] and 100% [24]; these assumptions gives an atomic density of $1.74\text{E}(22)$ [18] and $1.848\text{E}(22)$ [24] $^6\text{Li atoms-cm}^{-3}$. In this study the scintillator was modeled using a density of 3.494 g-cm^{-3} [25] and composed by 4.36 w/o of ^6Li , 0.18 w/o of ^7Li and 95.46 w/o of I. These characteristics give an atomic density of $1.523\text{E}(22)$ $^6\text{Li atoms-cm}^{-3}$.

Moderating spheres were modeled as 0.95 g-cm^{-3} polyethylene, that is the same to those used by other authors [18, 24], the element concentration features were taken from Seltzer and Berger [25]. Chemical binding and crystalline effects of polyethylene during thermal neutron scattering were taken into account using the $S(\alpha, \beta)$ treatment [20].

A disk-shaped source term with the same diameter as the moderating sphere was used to represent a monoenergetic neutron source whose neutrons were directed towards the polyethylene sphere.

Polyethylene spheres were modeled as a series of concentric polyethylene shells, each with a different neutron importance, increasing as the sphere center was approached. This was the only variance reduction technique used in this study.

Throughout the MCNP 4C and MCNPX calculations the number of histories used for each sphere was large enough to have uncertainties less than 3%. Finally, the calculated response functions were interpolated to include a larger number of energy bins; the set of these response functions is the BSS response matrix.

3. RESULTS AND DISCUSSION

In figure 1 the response functions for 0, 2, 3, 5, 8, 10, and 12 inches-diameter polyethylene spheres to neutrons from 2.5E(-8) to 100 MeV are shown.

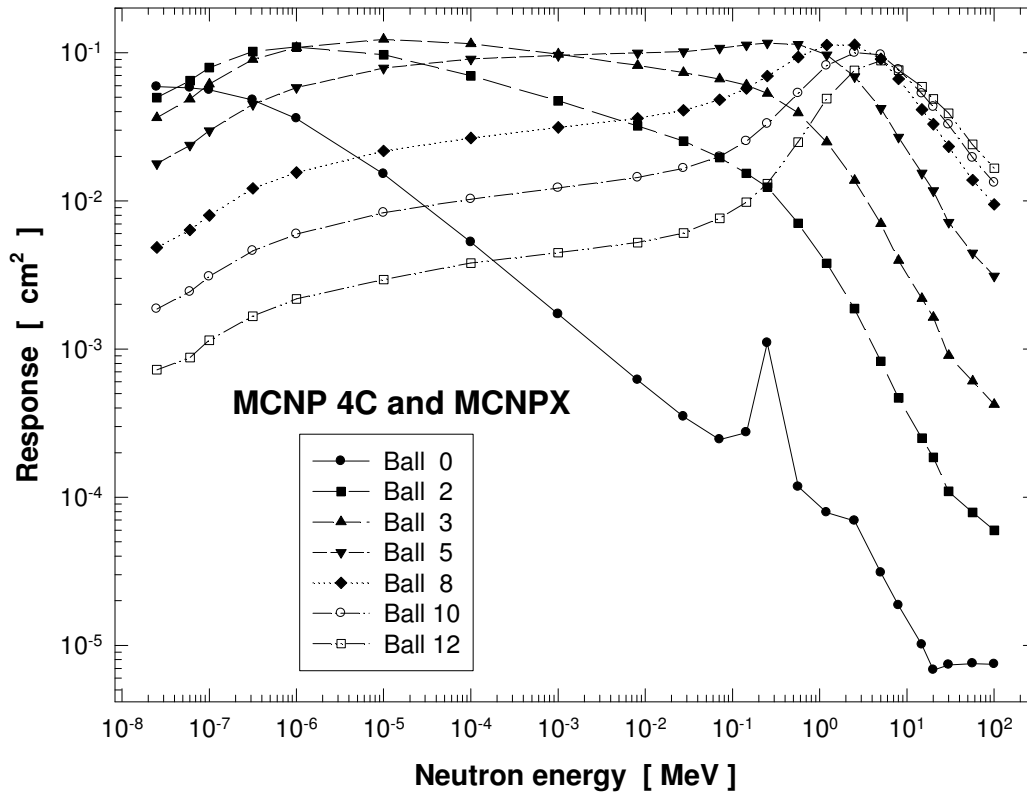


Figure 1. MCNP4C and MCNPX calculated response matrix for BSS with ⁶Li detector.

The bare detector (Ball 0) has the shape of ⁶Li cross section. As the sphere's diameter is increased the response tends to decrease for thermal and epithermal neutrons. On the other hand, the maximum in the responses is shifted to higher energies for larger-radii spheres. This behavior is in agreement to the response functions reported in the literature [17, 18] even regardless the type of thermal neutron detector [12, 15].

The energy-interpolated response functions are shown in Table I; this is the BSS/⁶LiI response matrix.

Table I. BSS/⁶Li energy-interpolated response functions, in (n,α) reactions per unit fluence

Neutron Energy [MeV]	Ball 0	Ball 2	Ball 3	Ball 5	Ball 8	Ball 10	Ball 12
1.000E-08	6.0166E-02	3.7778E-02	2.6774E-02	1.3145E-02	3.6364E-03	1.4114E-03	5.9382E-04
1.585E-08	5.9551E-02	4.3389E-02	3.1215E-02	1.5296E-02	4.1980E-03	1.6230E-03	6.5607E-04
2.512E-08	5.8942E-02	4.9833E-02	3.6391E-02	1.7798E-02	4.8463E-03	1.8663E-03	7.2483E-04
3.981E-08	5.8339E-02	5.7233E-02	4.2425E-02	2.0709E-02	5.5947E-03	2.1460E-03	8.0079E-04
6.310E-08	5.7628E-02	6.6051E-02	4.9767E-02	2.4236E-02	6.5017E-03	2.4884E-03	8.9879E-04
1.000E-07	5.6021E-02	7.9265E-02	6.1379E-02	2.9725E-02	7.9727E-03	3.0867E-03	1.1469E-03
1.585E-07	5.2590E-02	8.7640E-02	7.1491E-02	3.5025E-02	9.4336E-03	3.6191E-03	1.3317E-03
2.512E-07	4.9370E-02	9.6897E-02	8.3267E-02	4.1268E-02	1.1162E-02	4.2431E-03	1.5462E-03
3.981E-07	4.5161E-02	1.0329E-01	9.3267E-02	4.7188E-02	1.2756E-02	4.8397E-03	1.7578E-03
6.310E-07	4.0258E-02	1.0618E-01	1.0049E-01	5.2377E-02	1.4084E-02	5.3715E-03	1.9570E-03
1.000E-06	3.5889E-02	1.0915E-01	1.0828E-01	5.8135E-02	1.5549E-02	5.9616E-03	2.1787E-03
1.585E-06	3.0206E-02	1.0653E-01	1.1105E-01	6.1756E-02	1.6622E-02	6.3704E-03	2.3134E-03
2.512E-06	2.5424E-02	1.0398E-01	1.1390E-01	6.5601E-02	1.7769E-02	6.8070E-03	2.4564E-03
3.981E-06	2.1399E-02	1.0149E-01	1.1682E-01	6.9686E-02	1.8994E-02	7.2736E-03	2.6082E-03
6.310E-06	1.8010E-02	9.9052E-02	1.1981E-01	7.4027E-02	2.0305E-02	7.7724E-03	2.7695E-03
1.000E-05	1.5159E-02	9.6678E-02	1.2288E-01	7.8636E-02	2.1706E-02	8.3051E-03	2.9407E-03
1.585E-05	1.2267E-02	9.0583E-02	1.2123E-01	8.0902E-02	2.2593E-02	8.6635E-03	3.0962E-03
2.512E-05	9.9269E-03	8.4874E-02	1.1959E-01	8.3233E-02	2.3515E-02	9.0372E-03	3.2598E-03
3.981E-05	8.0335E-03	7.9525E-02	1.1798E-01	8.5631E-02	2.4475E-02	9.4270E-03	3.4321E-03
6.310E-05	6.5007E-03	7.4512E-02	1.1640E-01	8.8098E-02	2.5475E-02	9.8338E-03	3.6135E-03
1.000E-04	5.2608E-03	6.9816E-02	1.1483E-01	9.0636E-02	2.6515E-02	1.0258E-02	3.8045E-03
1.585E-04	4.2047E-03	6.4586E-02	1.1119E-01	9.1682E-02	2.7415E-02	1.0620E-02	3.9284E-03
2.512E-04	3.3607E-03	5.9749E-02	1.0766E-01	9.2739E-02	2.8345E-02	1.0994E-02	4.0564E-03
3.981E-04	2.6862E-03	5.5275E-02	1.0425E-01	9.3808E-02	2.9306E-02	1.1382E-02	4.1885E-03
6.310E-04	2.1469E-03	5.1134E-02	1.0094E-01	9.4891E-02	3.0300E-02	1.1783E-02	4.3249E-03
1.000E-03	1.7160E-03	4.7305E-02	9.7736E-02	9.5985E-02	3.1328E-02	1.2199E-02	4.4658E-03
1.585E-03	1.3710E-03	4.3414E-02	9.4010E-02	9.6782E-02	3.2309E-02	1.2645E-02	4.6234E-03
2.512E-03	1.0955E-03	3.9843E-02	9.0427E-02	9.7585E-02	3.3321E-02	1.3107E-02	4.7865E-03
3.981E-03	8.7529E-04	3.6566E-02	8.6980E-02	9.8395E-02	3.4365E-02	1.3586E-02	4.9554E-03
6.310E-03	6.9932E-04	3.3558E-02	8.3664E-02	9.9212E-02	3.5441E-02	1.4082E-02	5.1303E-03
1.000E-02	5.6094E-04	3.0750E-02	8.0375E-02	1.0000E-01	3.6824E-02	1.4714E-02	5.3609E-03
1.585E-02	4.5211E-04	2.8123E-02	7.7094E-02	1.0076E-01	3.8618E-02	1.5528E-02	5.6676E-03
2.512E-02	3.6441E-04	2.5720E-02	7.3947E-02	1.0152E-01	4.0500E-02	1.6387E-02	5.9917E-03
3.981E-02	3.0412E-04	2.2876E-02	7.0519E-02	1.0385E-01	4.3572E-02	1.7771E-02	6.6325E-03
6.310E-02	2.5586E-04	2.0214E-02	6.7158E-02	1.0662E-01	4.7157E-02	1.9396E-02	7.4212E-03
1.000E-01	2.5822E-04	1.7390E-02	6.3343E-02	1.0986E-01	5.2402E-02	2.2313E-02	8.6135E-03
1.585E-01	3.4817E-04	1.4762E-02	5.8994E-02	1.1317E-01	5.9325E-02	2.6507E-02	1.0293E-02
2.512E-01	1.0845E-03	1.2321E-02	5.3001E-02	1.1584E-01	6.9640E-02	3.3218E-02	1.3109E-02
3.981E-01	3.0664E-04	8.9717E-03	4.4608E-02	1.1451E-01	8.2253E-02	4.3417E-02	1.8897E-02
6.310E-01	1.1068E-04	6.4356E-03	3.6638E-02	1.1089E-01	9.5976E-02	5.6676E-02	2.7546E-02
1.000E+00	8.6742E-05	4.4043E-03	2.7858E-02	1.0056E-01	1.0773E-01	7.3660E-02	4.1574E-02
1.585E+00	7.4989E-05	2.9007E-03	1.9921E-02	8.5101E-02	1.1284E-01	8.8191E-02	5.7840E-02
2.512E+00	6.8811E-05	1.8614E-03	1.3676E-02	6.8754E-02	1.1279E-01	9.9898E-02	7.6141E-02
3.981E+00	4.0239E-05	1.0819E-03	8.7581E-03	4.9465E-02	9.7424E-02	9.7631E-02	8.4164E-02
6.310E+00	2.3994E-05	6.2360E-04	5.2873E-03	3.3680E-02	7.7704E-02	8.6222E-02	8.2189E-02
1.000E+01	1.4886E-05	3.6304E-04	3.1946E-03	2.1941E-02	5.5907E-02	6.7124E-02	6.9454E-02
1.585E+01	9.2312E-06	2.1957E-04	2.0500E-03	1.4443E-02	3.9210E-02	5.0513E-02	5.6410E-02
2.512E+01	7.1296E-06	1.3613E-04	1.1697E-03	8.8834E-03	2.7051E-02	3.6923E-02	4.2976E-02
3.981E+01	7.4437E-06	9.4532E-05	7.5551E-04	5.7866E-03	1.8426E-02	2.6001E-02	3.1406E-02
6.310E+01	7.5025E-06	7.4744E-05	5.6503E-04	4.1432E-03	1.2856E-02	1.8141E-02	2.2355E-02
1.000E+02	7.4532E-06	5.9766E-05	4.2188E-04	3.1005E-03	9.4667E-03	1.3249E-02	1.6594E-02

Energy-interpolated response functions were compared with those published by Mares and Schraube [18]. This comparison was carried out dividing the Mares and Schraube response

functions by a factor of 2.356262 (M and S, scaled). This scaling factor (k) was obtained according equation 3.

$$k = \frac{ad_{MS}}{ad} \frac{af_{MS}}{af} \tag{3}$$

Here, ad_{MS} , af_{MS} are the ⁶Li atomic density and the ⁶Li atomic fraction respectively, utilized by Mares and Scharube, ad and af are the ⁶Li atomic density and the ⁶Li atomic fraction respectively utilized in this work; this last is affected by the density utilized to model the scintillator.

In figures 2 to 8 are shown the response functions calculated in this study with the Mares and Schrabue multiplied by the scaling factor.

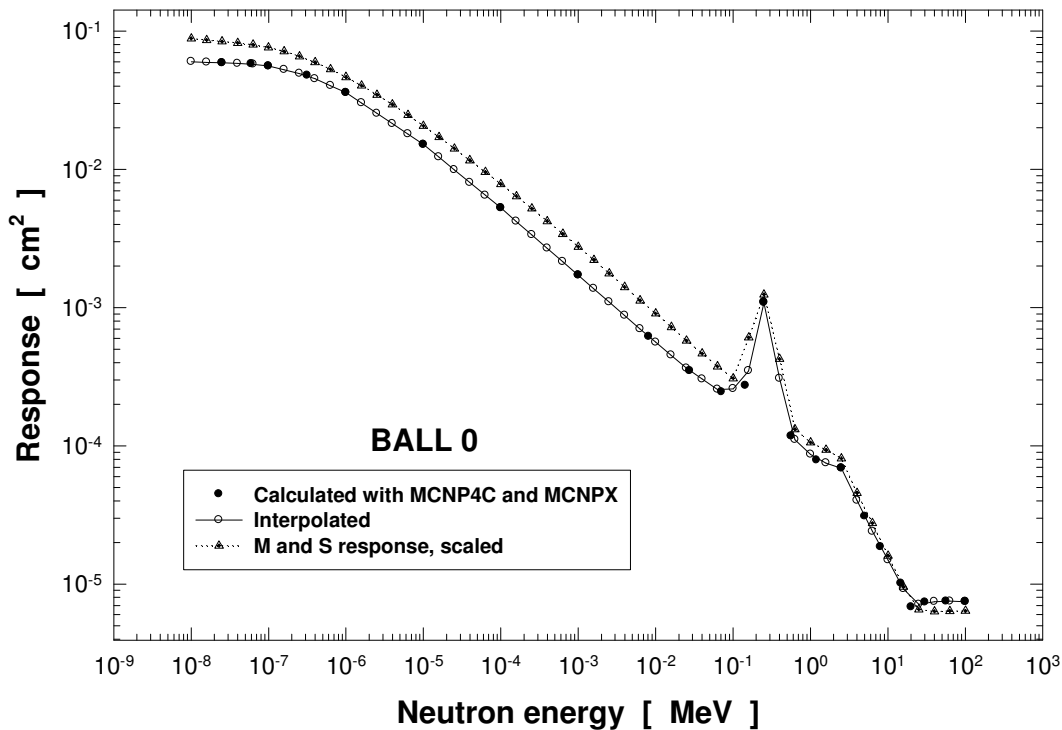


Figure 2. Bare detector's, calculated, interpolated and Mares and Schaubé, response function

In figure 2 can be noticed that, even when the M and S response function has been scaled by the k-factor, there is a difference in the region below the resonance (peak). The probable explanation is attributed to the different cross section libraries utilized and because for this detector Mares and Schraube did the calculation irradiating the bare detector laterally while in this work all irradiations were carried out with the neutron disk source centered on and perpendicular to the axis of the detector.

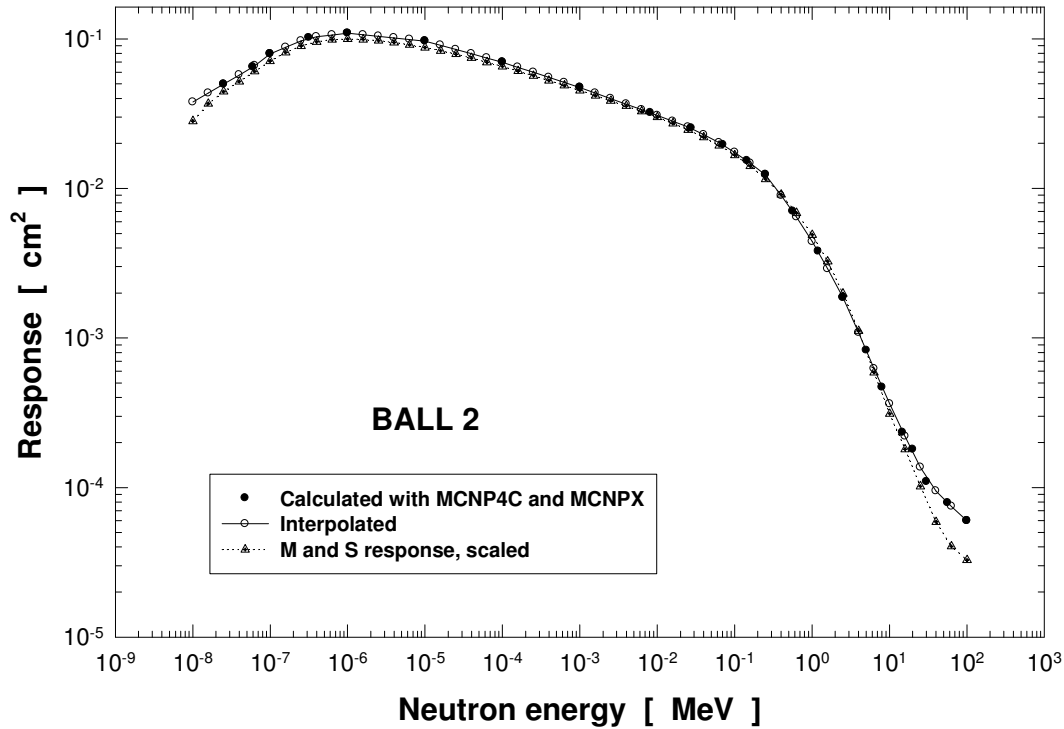


Figure 3. Ball 2 detector's, calculated, interpolated and Mares and Schraube response function.

For Ball 2 to Ball 12 the main differences are in the low energy region and for neutrons whose energy is larger to 20 MeV, i.e. those values calculated using MCNPX. Probable explanation of this difference is attributed to the cross sections utilized by Mares and Schraube for neutrons beyond 20 MeV. They utilized the HIGH library [18], while in this study it was utilized those included in MCNPX.

The chi-square test was applied to compare the response functions with the scaled Mares and Schraube response functions.

The test was applied using $\alpha = 0.95$ and 22 degrees of freedom; for these parameters the χ^2 -critical value is 12.3338. The calculated chi-square values for each detector are shown in Table II. Using this test it can be noticed that all the calculated chi-values are smaller than the critical chi-value. This mean that there are not significant differences between the response functions calculated in this work and those reported by Mares and Schraube scaled by the k-factor.

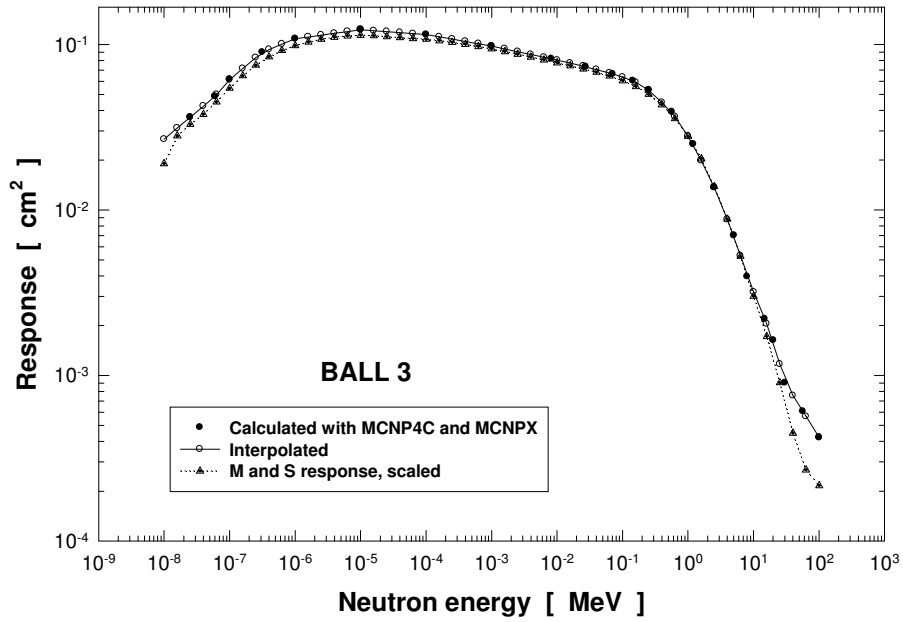


Figure 4. Ball 3 detector's, calculated, interpolated and Mares and Schaube response function.

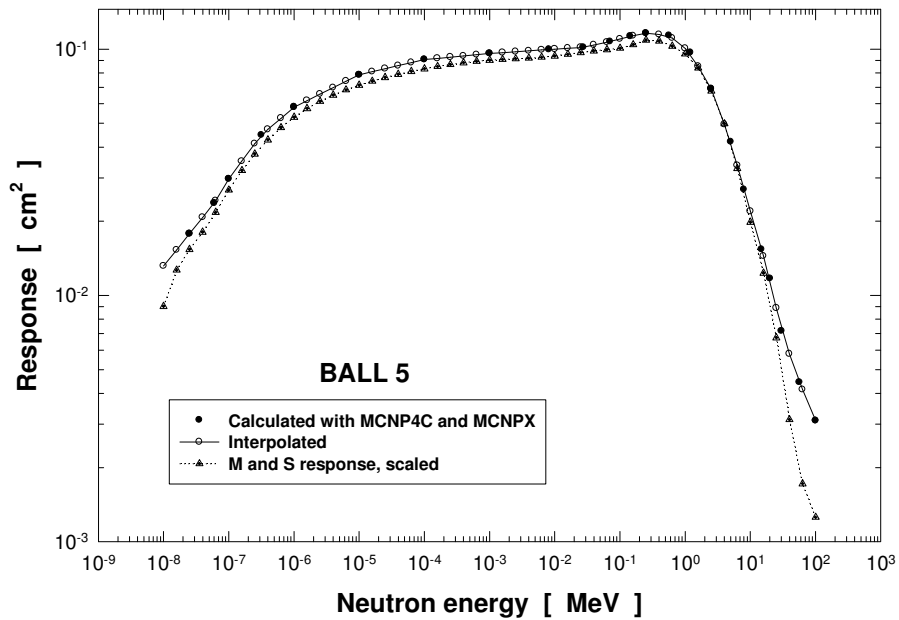


Figure 5. Ball 5 detector's, calculated, interpolated and Mares and Schaube response function.

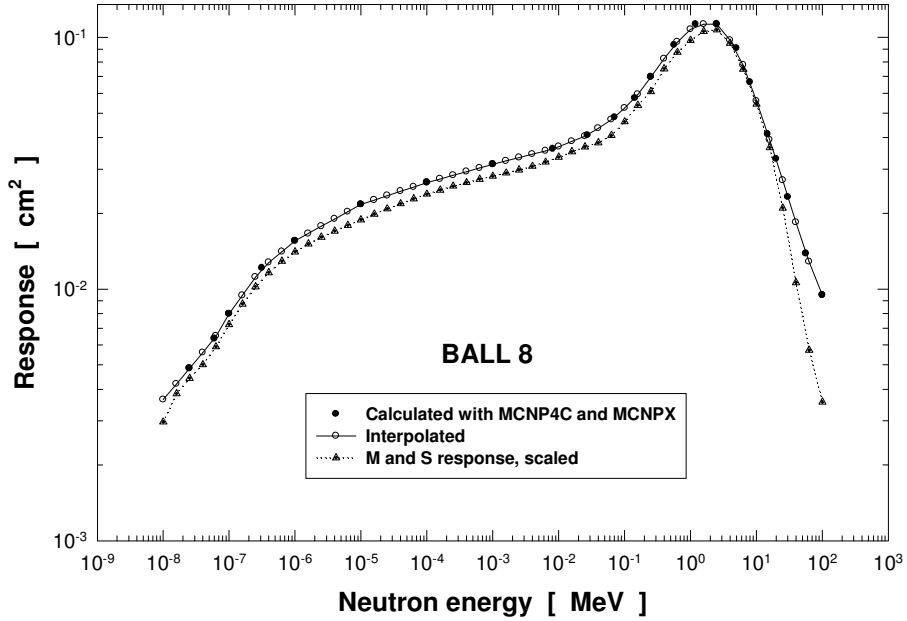


Figure 6. Ball 8 detector's, calculated, interpolated and Mares and Schaubé response function.

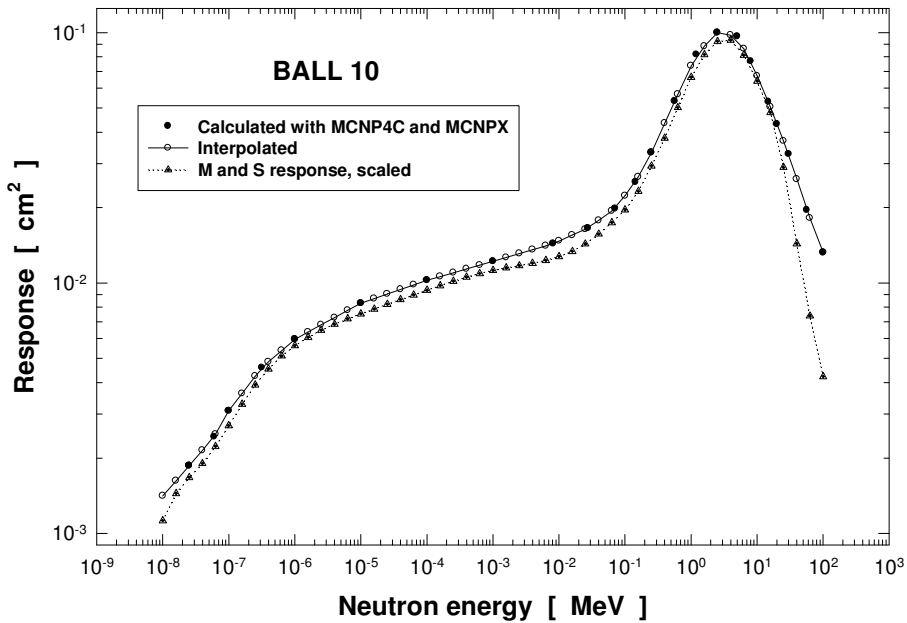


Figure 7. Ball 10 detector's, calculated, interpolated and Mares and Schaubé response function.

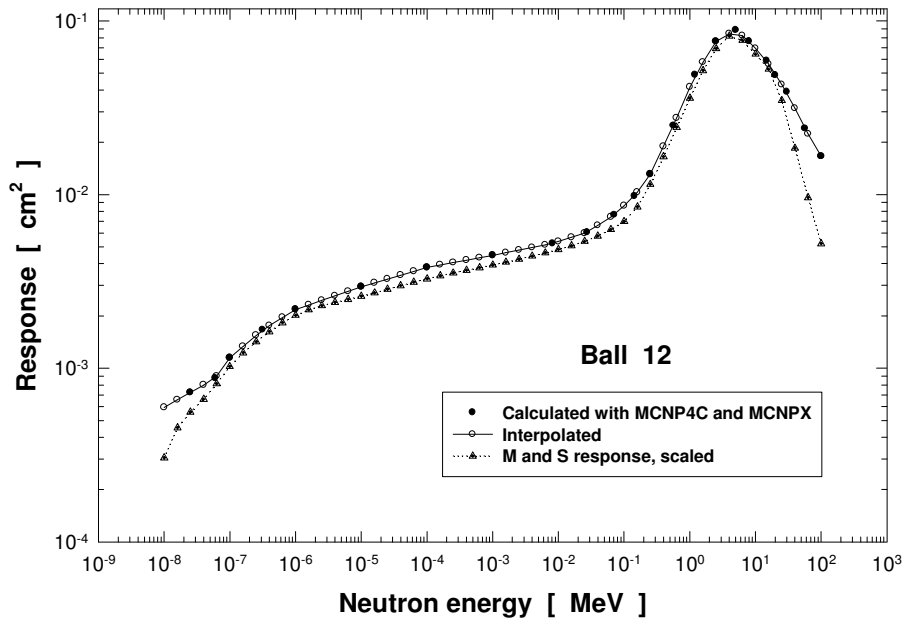


Figure 8. Ball 12 detector's, calculated, interpolated and Mares and Schaub response function.

Table II. Calculated Chi-square

Detector	χ^2
Ball 0	8.1657E(-2)
Ball 2	1.6961E(-2)
Ball 3	1.8753E(-2)
Ball 5	2.9715E(-2)
Ball 8	4.2383E(-2)
Ball 10	5.5891E(-2)
Ball 12	5.9984E(-2)

4. CONCLUSIONS

The fluence responses for seven Bonner spheres have been calculated for neutrons from 2.50E(-8) to 100 MeV. For neutron from 2.50E(-8) to 20 MeV calculations were carried out using the MCNP 4C and the ENDF/B-VI cross-section library. For neutrons from 30 to 100 MeV the response was calculated with the MCNPX code and the LA150 cross section library. For all the calculated cases where the polyethylene spheres are included the $S(\alpha, \beta)$ scattering model was utilized to include the physics of low energy neutrons transport.

Response functions were calculated for 23 energy bins and were interpolated to include a larger number, thus the response matrix was obtained for 51 energy bins.

Good agreement was observed between our response matrix and the matrix calculated by other scientists [2, 8, 11, 12, 15, 17, 18, 19, 24]. Response functions are similar in shape regardless of thermal neutron detector and the method utilized to do the calculations except for the bare detector (Ball 0) case where its response is strongly influenced by the type of thermal neutron detector.

The response functions were compared with those reported by Mares and Schraube, before to make the comparisons their response functions were scaled by a k-factor that includes the atomic density and the atomic fractions utilized by Mares and Schraube and those utilized in this work.

Comparing the response function for Bare detector with the scaled response function of Mares and Schruabe differences are observed due to the irradiation conditions utilized during calculations and the cross sections libraries. For the other detectors the differences are mainly observed in the low energy region and in the case of neutrons whose energy is larger to 20 MeV; this is attributed to the different cross sections libraries utilized in both studies. The chi-square test was applied to determine if there are significant differences between our response functions and those, scaled by the k-factor, reported by Mares and Schraube. From this test no significant differences were observed.

The need to use k-factor means that all the previous response matrices are larger than those here calculated; this implies that the neutron spectra calculated with the old responses are over responded.

ACKNOWLEDGMENTS

This work is part of the SYNAPSIS project supported by CONACyT (México) under contract SEP-2004-C01-46893.

REFERENCES

1. Chadwick, J., "Possible existence of a neutron", *Nature*, **129** p.312 (1932).
2. Bramblett, R.L., Ewing, R.I. and Bonner, T.W., "A new type of neutron spectrometer", *Nuclear Instruments and Methods*, **9** p. 1-12 (1960).
3. Brooks, F.D. and Klein, H., "Neutron spectrometry-historical review and present status", *Nuclear Instruments and Methods in Physics Research A* **476**, p. 1-11 (2002).
4. Kralik, M., Aroua, A., Grecescu, M., Mares, V., Novotny, T., Schraube, H. and Wiegel B., "Specification of Bonner sphere systems for neutron spectrometry", *Radiation Protection Dosimetry*, **70** p. 279-284 (1997).
5. Sannikov, A.V., Mares, V. and Schraube, H., "High energy response functions of Bonner spectrometers", *Radiation Protection Dosimetry*, **70** p. 291-294 (1997).
6. Vylet, V., "Response matrix of an extended Bonner sphere system", *Nuclear Instruments and Methods in Physics Research A* **476**, p. 26-30 (2002).
7. Gallego, E., Lorente, A. and Vega-Carrillo, H.R., "Characteristics of the neutron field of the facility at DIN-UPM", *Radiation Protection Dosimetry* **110** , p. 73-79 (2004).

8. Vega-Carrillo, H.R., “TLDs pairs, as thermal neutron detectors in neutron multisphere spectrometry”, *Radiation Measurements* **35**, p. 251-254 (2002).
9. Sweezy, J.E., Hertel, N.E., Veinot, K.G. and Karam, R.A., “Performance of multisphere spectrometry systems”, *Radiation Protection Dosimetry* **78**, p. 263-272 (1998).
10. Barquero, R., Méndez, R., Iñiguez, M.P., Vega-Carrillo, H.R. and Voytchev, M., “Thermoluminescence measurements of neutron dose around a medical linac”, *Radiation Protection Dosimetry*, **101**, p. 493-496 (2002).
11. Thomas, D.J., Bardell, A.G. and Macaulay, E.M., “Characterisation of a gold foil-based Bonner sphere set and measurements of neutron spectra at a medical accelerator”, *Nuclear Instruments and Methods in Physics Research A*, **476**, p. 31-35 (2002).
12. Dhairyawan, M.P., Nagarajan, P.S. and Venketaraman, G., “Further studies on the response of spherical moderated neutron detectors”, *Nuclear Instruments and Methods*, **175**, p. 561-564 (1980).
13. Alevra, A.V. and Thomas, D.J., “Neutron spectrometry in mixed fields: Multisphere spectrometers”, *Radiation Protection Dosimetry*, **107**, p. 37-72 (2003).
14. Wiegel, B. and Alevra, A.V., “NEMUS-The PTB Neutron Multisphere Spectrometer: Bonner spheres and more”, *Nuclear Instruments and Methods in Physics Research A*, **476**, p. 36-41 (2002).
15. Vega-Carrillo, H.R., Manzanares-Acuña, E., Hernandez-Dávila, V.M. and Mercado, G.A., “Response matriz of a multisphere neutron spectrometer with an ^3He proportional counter”, *Revista Mexicana de Física*, **51**, p. 47-52 (2005).
16. Vega-Carrillo, H.R., Manzanares-Acuña, E., Hernandez-Dávila, V.M. and Mercado, G.A., Gallego, E. y Lorente, A. “Características dosimétricas de fuentes isotópicas de neutrons”, *Revista Mexicana de Física*, **51**, p. 494-501 (2005).
17. Hertel, N.E. and Davidson, J.W., “The response of Bonner spheres to neutrons from thermal energies to 17.3 MeV”, *Nuclear Instruments and Methods in Physics Research A*, **238**, p. 509-516 (1985).
18. Mares, V. and Schraube, H., “Evaluation of the response matrix of a Bonner spheres spectrometer with LiI detector from thermal energy to 100 MeV”, *Nuclear Instruments and Methods in Physics Research A*, **337**, p. 461-473 (1994).
19. Vega-Carrillo, H.R., Wehring, B.W., Veinot, K.G. and Hertel, N.E., “Response matrix for a multisphere spectrometer using ^6LiF thermoluminescence dosimeter”, *Radiation Protection Dosimetry*, **81**, p. 133-140 (1999).
20. Briesmeister, J.F. (editor), *MCNPTM-A general Monte Carlo N-particle transport code*, Los Alamos National Laboratory **Report LA-13709-M** (2000).
21. Hendricks, J.S., Frankle, S.C. and Court, J.D., *ENDF/B-VI Data for MCNPTM*, Los Alamos National Laboratory **Report LA-12891** (1994).
22. Waters, L.S. (editor), *MCNPX User's manual version 2.4.0*. Los Alamos National Laboratory **Report LA-CP-02-408** (2002).
23. Chadwick, M.B., Young, P.G., Chiba, S., Frankle, S., Hale, G.M., Hughes, H.G., Koning A.J., Little, R.C., MacFarlane, R.E., Prael, R.E., Waters, L.S., “Cross sections evaluations to 150 MeV for accelerator-driven systems and implementation in MCNPX”, *Nuclear Science and Engineering*, **131**, p. 293-328 (1999).
24. Lemley, E., *Calculation of Bonner sphere neutron spectrometer response functions using the Monte Carlo computer code MCNP*. **PhD dissertation. University of Arkansas** (1996).

25. Seltzer, S.M. and Berger, M.J., "Evaluation of the collision stopping power of elements and compounds for electrons and positrons", *International Journal of Applied Radiation and Isotopes*, **33**, p. 1189-1218 (1982).